DETERMINATION OF OVERALL KINETIC RATES AND OXYGEN REACTION ORDER FOR SARAN CHAR COMBUSTION

B.J. Waters, R.E. Mitchell*, R.G. Squires and N.M. Laurendeau

Purdue University, West Lafayette, IN 47907
* - Sandia National Laboratories, Livermore, CA 94550

Introduction

Recent work by Mitchell and co-workers [1,2,3] on a novel entrained flow reactor has demonstrated the feasibility of extracting kinetic rate parameters from the simultaneous measurement of the temperature, diameter and velocity of individual coal particles. These rate parameters are obtained by solving the conservation equations for a coal particle as it burns in a laminar, coflowing gas stream. In this analysis, assumptions must be made about the devolatilization processes which occur during particle heatup. Specifically, the char density, ash composition and heat gain of the particle due to homogeneous combustion of volatiles become parameters in the reactor model that depend on the parent coal.

In this work, the entrained flow reactor is used to investigate the combustion of Saran char, a very low ash, high surface area, amorphous carbon. The highly irregular Saran char particles offer a coal analog without the complicating effects associated with devolatilization and catalytic impurities. We report overall particle burning rates, apparent rate coefficients, and the apparent reaction order with respect to oxygen.

Experimental Procedure

The combustion of Saran char particles is followed in a transparent, rectangular, entrained flow reactor which is described in detail elsewhere [4]. Briefly, the particles are entrained in a cold N_2 stream and are then injected along the centerline at the base of the 40 cm high reactor. Particle loadings are kept low to insure that their presence has no influence on the free-stream gas properties. A two-color pyrometer is used to measure the temperature of the burning particles at discrete heights in the reactor. As the particle traverses the focal volume of the collection optics, the radiant emission passes through two different sized slits. The first slit is wider (1000 μm) than the diameter of the largest particle and the second is narrower (45 μm) than the diameter of the smallest particle. The ratio of the intensity of the radiant emission measured in the first slit to that measured in the second slit is directly proportional to the diameter of the particle. The temperature measurements are calibrated with a tungsten strip lamp; the size measurements are calibrated by comparison with the size distribution of well-characterized Spherocarb particles. The particle temperatures measured in this work ranged from 1440 ±20 K in 12 kPa O_2 to 2100 ±150 K in 36 kPa O_2. The measured particle diameters ranged from 80 to 170

μm which corresponds well with the -100/+170 mesh (90-150 μm) particles used to feed the reactor. The velocity of each particle is determined by measuring the time it takes the particle to traverse the large slit. The particle velocities measured in this work ranged from 2.40 to 3.10 (±0.05) m/s depending on the gas temperature.

To reduce the influence of spurious signals, 200 to 300 particles were monitored at each height and the particles were grouped in bins approximately 10 μm apart, based on their measured diameter. In this paper, a measured particle diameter refers to the diameter at the center of a bin containing at least 10 particles. A measured particle temperature or velocity refers to the average temperature or velocity for all of the particles in a given bin.

A hot, one-dimensional, laminar oxidizing gas environment is generated by a 5 cm x 5 cm array of 0.2 cm diameter $CH_4/H_2/O_2/N_2$ diffusion flamelets. The total pressure in the reactor is constant and equal to 101 kPa. Post flame O_2 partial pressures from 3 to 36 kPa and gas temperatures from 1400 to 1900 K are attained by careful control of the inlet gas mixture. During analysis of the experimental data, we found that Saran char had a negligible burning rate in 3 and 6 kPa O_2 environments. Therefore, in the remainder of this paper, we only present data obtained at 12, 24, and 36 kPa O_2. Typical post flame partial presures of H_2O and CO_2 are 16 and 2 kPa, respectively.

Gas temperatures, T_g, are determined from radiation-corrected measurements using a Pt-Pt/13%Rh thermocouple. The gas velocity in the reactor can be modeled as,

$$\sqrt{\frac{\overline{v_g}}{T_g}} = C_1 + 0.5\sqrt{\overline{C_2 z T_g^{0.68}}} + \frac{C_2 z T_g^{0.68}}{8\sqrt{\overline{C_1}}} \qquad (1)$$

where z is the height in the reactor, C_1 and C_2 are constants that are fit to the data for each gas condition, and the two $T_g^{0.68}$ terms account for the influence of T_g on the gas viscosity. Eqn. (1) represents the solution of the conservation equation governing one-dimensional flow in a square conduit, assuming that the boundary layer along each wall develops independently and that the fraction of the total mass flowing in the boundary layer is proportional to the boundary layer thickness. C_1 and C_2 are chosen to give the best fit between the measured particle velocities and the particle velocities calculated by solving the particle momentum balance (see Eqn. (3) below). An important implicit assumption in this analysis is that the density of the particles are approximately independent of burning time. This assumption is consistent with the results of the kinetic analysis discussed below.

The Saran char is made by heating Saran co-polymer (supplied by the Dow Chemical Company) to 1300 K in flowing N_2 for three hours. The exact procedure used to manufacture the Saran char is described elsewhere [5]. Saran char contains no volatiles and approximately 0.5 wt% ash. Its apparent bulk density is 0.35 g/ml and its total surface

area is 1260 m^2/g, as determined by CO_2 adsorption at 298 K analyzed using the Dubinin-Radushkevich isotherm. The only impurities detected by Proton Induced X-ray Emission Spectroscopy (PIXE) are 2300 ppm Cl, 22-30 ppm Ti, 10 ppm Fe, 7.2 ppm Cu, 1 ppm Zr, and 1 ppm Re.

Theory

The equations used to follow the mass, velocity and temperature of a particle as it burns in the laminar flow reactor are given below:

$$v_p \frac{dm}{dz} = -\rho \pi d_p^2 \tag{2}$$

$$m v_p \frac{dv_p}{dz} = -mg - 3\pi \mu d_p (v_p - v_g) \tag{3}$$

$$\frac{-m v_p C_p}{\pi d_p^2} \frac{dT_p}{dz} + \rho H = \frac{2k(T_p - T_g)}{d_p} + \sigma \varepsilon_p (T_p^4 - T_w^4) \tag{4}$$

The momentum equation (Eqn. (3)) accounts for gravitational and Stokes forces and the energy balance (Eqn. (4)) accounts for the thermal inertia of the particle, the heat of reaction, gas phase conduction, and radiation. The mass, m, of the char particle is determined from its apparent density and diameter, d_p. The particle velocity is v_p and ρ is the particle burning rate per unit external surface area. The velocity of the gas is given by v_g and g is the gravitational constant. The heat capacity of the particle, C_p, is taken to be that of graphite and the physical properties of N_2, the major component in the gas stream, are used for the free-stream gas properties. The viscosity, μ, and thermal conductivity, k, of the gas are evaluated at the mean temperature (T_m) between the gas and particle temperatures. The temperatures of the particle, the gas, and the medium to which the particle radiates are given by T_p, T_g and T_w (500 K), respectively. The Stefan-Boltzmann constant is denoted by σ, and ε_p denotes the particle emissivity (taken as 0.85). The heat released per gram of carbon consumed, H, is calculated assuming that CO is the primary combustion product.

The overall burning rate of the particle is described by:

$$\rho = k_d (P_g - P_s) = k_s P_s^n, \tag{5}$$

where P_g and P_s are the oxygen partial pressures in the bulk stream and at the surface of the particle, respectively, k_s and k_d are the chemical rate and diffusion coefficients, respectively, and n is the apparent oxygen reaction order. The chemical reaction rate coefficient includes contributions from intraparticle diffusion limitations and the intrinsic reactivity of the Saran particle. In the Arrhenius form, k_s is given as,

$$k_s = A \exp(\frac{-E}{RT_p}), \quad (6)$$

where A is the preexponential factor, E is the activation energy, and R is the universal gas constant. The external diffusion rate coefficient is given by:

$$k_d = \frac{2M_c D_{ox}}{RT_m d_p}, \quad (7)$$

where M_c is the molecular weight of carbon and D_{ox} is the diffusion coefficient of oxygen evaluated at T_m.

The computational scheme employed to obtain the overall particle burning rate parameters, A, E, and n, is initiated by setting dT_p/dz equal to zero in Eqn. (4) and then using the measured d_p and T_p to calculate ρ. Using Eqns. (5) and (7), P_s can be calculated from ρ. The rate parameters are then obtained from Eqns. (5) and (6) by fitting T_p and P_s to the calculated rate using a linear least-squares routine. These parameter values are used as the first guess in the numerical integration of Eqns. (2), (3) and (4), where ρ is obtained from an implicit expression which is independent of P_s by rearrangement of Eqn. (5). The integration employs the measured T_g profile. The initial conditions used for the integration are T_p = 300 K and v_p = 0.3 m/s. A range of initial particle diameters (from 90 μm to 190μm) in 5 μm intervals is used. When the integration reaches a height (z) where experimental measurements have been taken, the calculated relationship between dT_p/dz and d_p is used to find dT_p/dz for each measured particle size. This measured dT_p/dz is then used in Eqn. (4) to obtain a new ρ, from which updated values of the kinetic parameters are obtained for the next numerical integration. Successive iterations of this strategy are used to converge on the rate parameter values that best describe the behavior of the Saran particles. The quality of fit can be judged from the agreement between the calculated and measured T_p as a function of d_p. Both constant density and constant diameter burning are considered as limiting cases for effectiveness factors of approximately zero and one respectively. The particle ignition temperature is taken as 1000 K below which the particle burning rate is set equal to zero. Changing the ignition temperature from 300 K to 1100 K does not affect the results of this analysis.

Results and Discussion

Equations (2), (3) and (4) can be solved to calculate the predicted relationship between particle temperature and size for a given gas environment. For the 12 kPa O_2 environments at a peak gas temperature less than 1700 K and in all O_2 environments less than 12 kPa, the measured particle temperatures can be fit by setting ρ equal to zero. This is in direct contrast to the burning characteristics of an hvb-bituminous coal observed by Mitchell and co-workers [2], which exhibited appreciable reaction rates in O_2 environments as low as 3 kPa. This may be attributed to two factors: (1) the homogeneous combustion of the volatile matter (33% by weight) in the coal

increases the temperature of the resulting char and (2) the catalytic properties of the ash (21% by weight) increase the burning rate of the char.

If the measured particle temperature does not exceed the calculated zero-burning temperature by the approximate error in our temperature measurement (±20-150 K), we can not calculate a statistically significant burning rate. Defining χ as the ratio of the calculated burning rate to the diffusion-limited burning rate ($\chi=\rho/k_d P_g$), we observed that the difference in particle temperature between χ's of 0.0 and 0.1 approximately corresponds to the error in the measured particle temperature. Therefore, no measurements which give a χ below 0.1 are considered in the determination of the rate coefficients and oxygen reaction order. For the conditions of these experiments, values of χ ranged from 0.1 to 0.6 which indicates that the overall burning rate has a high sensitivity to the kinetic rate.

For an O_2 partial pressure of 36 kPa, 100 μm particles are predicted to burn out at approximately 10 cm in the reactor, if constant diameter burning is assumed. This contradicts the experimental observation of particles as small as 90 μm at 19 cm in the reactor. While a constant diameter model may be more applicable at lower O_2 pressures, this model was not used in our analysis of the combustion kinetics. An analysis incorporating an effectiveness factor into the particle burning rate expression will be considered in future work.

Constant density burning gives good fits to the experimental data at bulk oxygen pressures of 12 and 24 kPa and poor fits to the 36 kPa data (see Figures 1, 2 and 3). A least squares fit of the kinetic rate parameters and oxygen reaction order to the calculated reaction rates at 12, 24 and 36 kPa gives

$$\rho = 6.3\times10^{-3} \exp\left(\frac{-27000}{RT_p}\right) P_s^{0.8} \qquad (8)$$

where R is given in cal/mol K and P_s is given in Pa. An Arrhenius plot of the rate coefficient, k_s, versus $1/T_p$ is presented in Figure 4. The relationship between (ρ/k_s) and P_s is depicted in Figure 5.

A possible reason for the discrepancy between the calculated and experimental rates for the 36 kPa data set is that the simple diffusion model considered here does not account for the large amount of CO which must diffuse out of the particle boundary layer at higher burning rates (Stefan flow). We do note, however, that when the 36 kPa data is analyzed alone, the calculated rates fit the data better, but the activation energy is lower (~17000 cal/mol) which is indicative of intraparticle diffusion limitations.

Acknowledgements

The experimental work was performed at the Combustion Research Facility, Sandia National Laboratories and was sponsored by the U.S. Dept. of Energy through PETC. The computational work was performed at

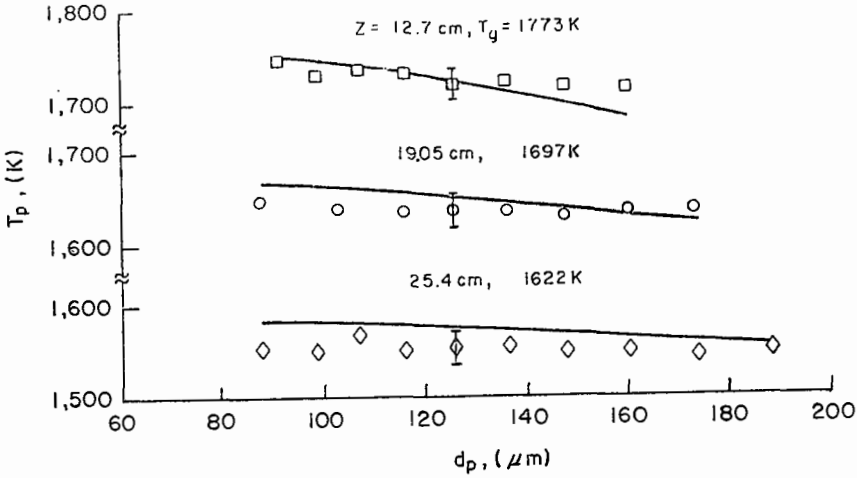

Figure 1. Particle temperature versus diameter as a function of height in the reactor. Free stream oxygen pressure is 12 kPa. (χ = 0.1-0.3)

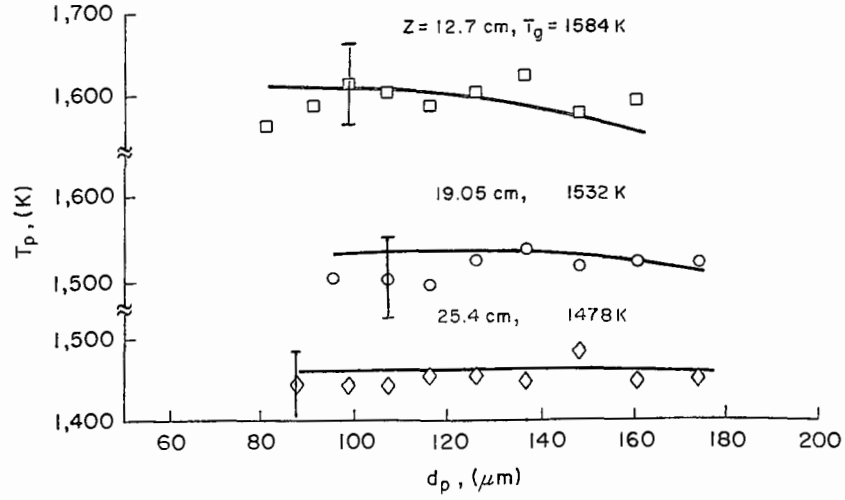

Figure 2. Particle temperature versus diameter as a function of height in the reactor. Free stream oxygen pressure is 24 kPa. (χ = 0.1-0.3)

the Purdue University Computing Center and was sponsored by the Coal Research Center at Purdue University. B.J.W. acknowledges the support provided by the D.O.E. through Associated Western Universities.

References

1. Mitchell, R.E., Tichenor, D.A. and Hencken, K.R., Proceedings of the 1985 International Conference on Coal Science, International Energy Agency, 1985, p.375.

2. Mitchell, R.E., Tichenor, D.A. and Hencken, K.R., Second Annual Pittsburgh Coal Conference Proceedings, Pittsburgh, Sept. 16-20, 1985, p.648.

3. Tichenor, D.A., Mitchell, R.E., Hencken, K.R., and Niksa, S. Twentieth Symposium (Int.) on Combustion, Ann Arbor, Aug. 12-17, 1984.

4. Hardesty, D.R., Pohl, J.A. and Stark, A.H., Sandia Report SAND78-8234, Sandia National Laboratories, Livermore, CA, 1978.

5. Waters, B.J., M.S. Thesis, Purdue University, 1985.

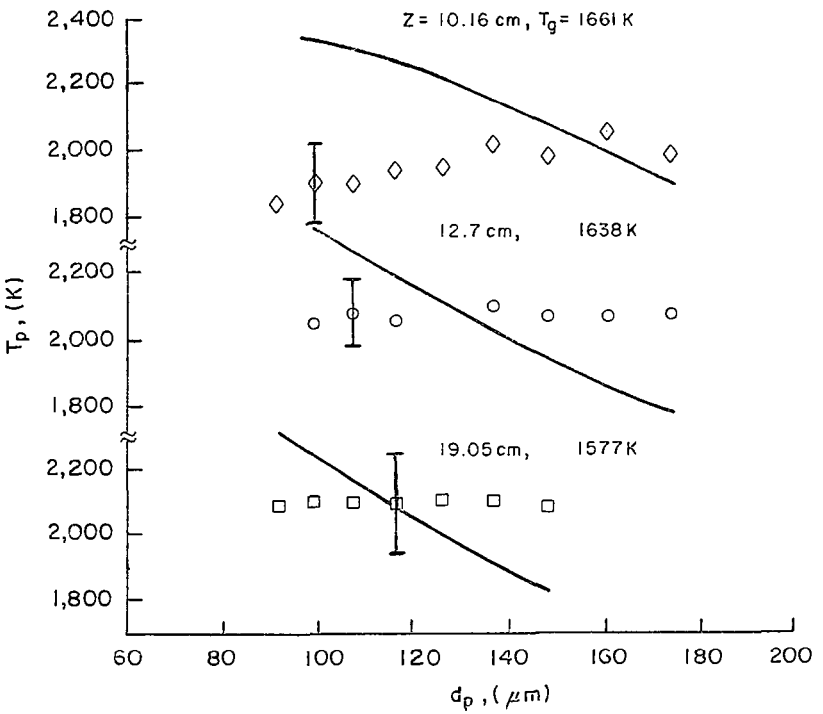

Figure 3. Particle temperature versus diameter as a function of height in the reactor. Free stream oxygen pressure is 36 kPa. (χ = 0.3-0.6)

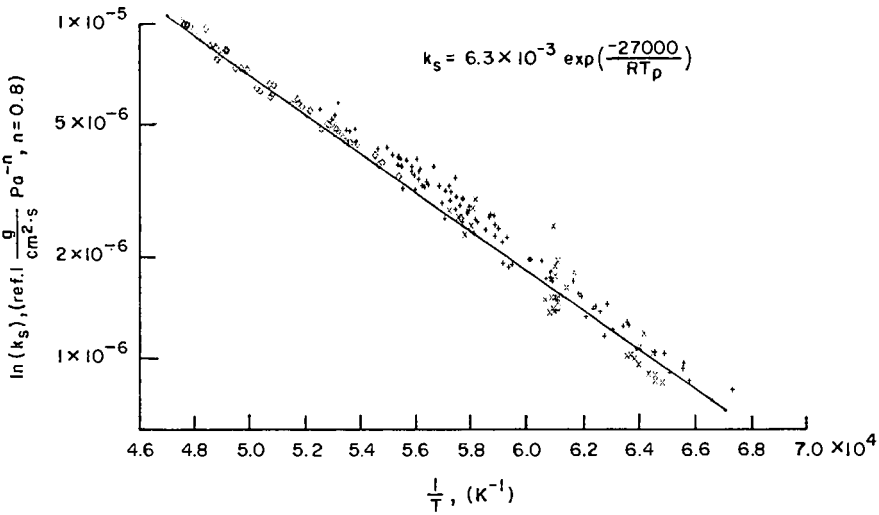

Figure 4. Temperature dependence of k_s.
Free stream oxygen: ◇ - 36 kPa; + - 24 kPa; × - 12 kPa.

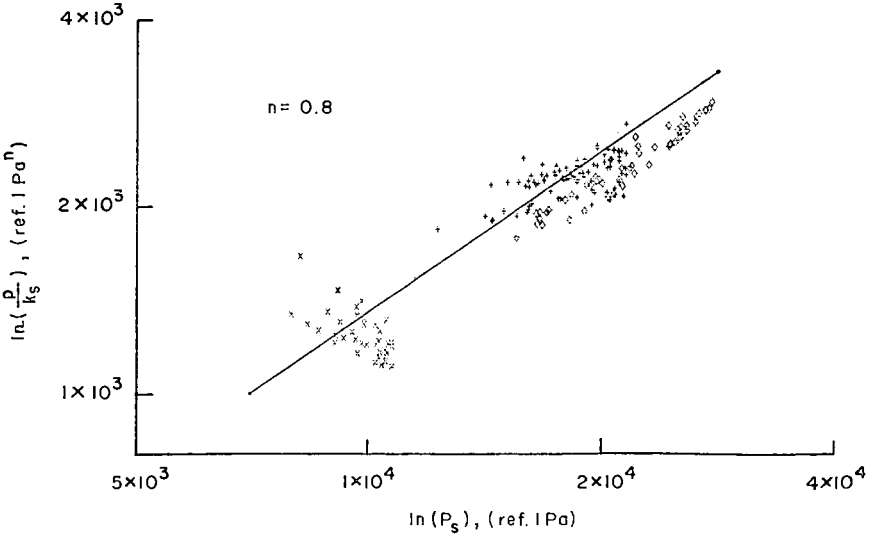

Figure 5. Surface oxygen pressure dependence of $\frac{p}{k_s}$.
Free stream oxygen: ◇ - 36 kPa; + - 24 kPa; × - 12 kPa.